AAS 15-634

ENGINEERING MESSENGER'S GRAND FINALE AT MERCURY – THE LOW-ALTITUDE HOVER CAMPAIGN

James V. McAdams[*], Christopher G. Bryan[†], Stewart S. Bushman[‡], Andrew B. Calloway[§], Eric Carranza[**], Sarah H. Flanigan[††], Madeline N. Kirk[‡‡], Haje Korth[§§], Dawn P. Moessner[***], Daniel J. O'Shaughnessy[†††], and Kenneth E. Williams[‡‡‡]

Having completed its primary and first extended missions by mid-March 2013, the MESSENGER spacecraft in orbit about Mercury began a 2.1-year final mission extension that brought substantial opportunity for low-altitude science, along with many technical challenges successfully overcome by the flight operations and science teams. After four orbit-correction maneuvers (OCMs) between June 2014 and January 2015 targeted minimum altitudes near 25 km and 15 km, seven OCMs in March and April 2015 maintained minimum altitude between 5 km and 37 km. Engineering challenges at mission end included the efficient utilization of accessible propellant and helium gas pressurant to delay Mercury impact.

INTRODUCTION

Designed and operated by The Johns Hopkins University Applied Physics Laboratory (JHU/APL) in Laurel, Maryland, the MErcury Surface, Space ENvironment, GEochemistry, and Ranging (MESSENGER) spacecraft became the first orbiter of the planet Mercury on 18 March

[*] MESSENGER Mission Design Lead Engineer, The Johns Hopkins University Applied Physics Laboratory, 11100 Johns Hopkins Rd., Laurel, MD 20723.
[†] MESSENGER Navigation Team Chief, KinetX Aerospace, Space Navigation and Flight Dynamics, Tempe, AZ 85284.
[‡] MESSENGER Propulsion Lead Engineer, The Johns Hopkins University Applied Physics Laboratory, 11100 Johns Hopkins Rd., Laurel, MD 20723.
[§] MESSENGER Mission Operations Manager, The Johns Hopkins University Applied Physics Laboratory, 11100 Johns Hopkins Rd., Laurel, MD 20723.
[**] MESSENGER Lead Orbit Determination Analyst, KinetX Aerospace, Space Navigation and Flight Dynamics, 123 W. Easy St., Simi Valley, CA 93065.
[††] MESSENGER Guidance and Control Lead Engineer, The Johns Hopkins University Applied Physics Laboratory, 11100 Johns Hopkins Rd., Laurel, MD 20723.
[‡‡] MESSENGER Guidance and Control Lead Analyst, The Johns Hopkins University Applied Physics Laboratory, 11100 Johns Hopkins Rd., Laurel, MD 20723.
[§§] MESSENGER Deputy Project Scientist, The Johns Hopkins University Applied Physics Laboratory, 11100 Johns Hopkins Rd., Laurel, MD 20723.
[***] MESSENGER Mission Design Lead Analyst, The Johns Hopkins University Applied Physics Laboratory, 11100 Johns Hopkins Rd., Laurel, MD 20723.
[†††] MESSENGER Mission Systems Engineer, The Johns Hopkins University Applied Physics Laboratory, 11100 Johns Hopkins Rd., Laurel, MD 20723.
[‡‡‡] Mission Director - Navigation, KinetX Aerospace, Space Navigation and Flight Dynamics, 123 W. Easy St., Simi Valley, CA 93065.

2011 UTC. Supported by NASA's Discovery Program, the spacecraft successfully completed its 7.6-year primary mission on 17 March 2012. The MESSENGER mission recently concluded operations after completing its final seven mission-extending, periapsis-raising maneuvers during the mission's final extended mission phase. The primary mission phases for MESSENGER were: (1) a 6.6-year interplanetary cruise beginning with a 3 August 2004 launch followed by one Earth flyby, two Venus flybys, and three Mercury flybys, culminating in Mercury orbit insertion[1] (MOI), and (2) one year in a near-polar, high-eccentricity, 200–500-km periapsis altitude, 12-h period orbit around Mercury with six orbit-correction maneuvers (OCMs)[2]. The extended mission phases included: (1) a first extended mission (XM1) from 18 March 2012 through 17 March 2013, with two OCMs that together lowered the orbit period to 8 h for the final 11 months of XM1, (2) a second extended mission (XM2) from 18 March 2013 to 18 March 2015 with four OCMs[3], and (3) a slight, final extension of XM2 (XM2′) with seven OCMs between 18 March 2015 and a high-speed Mercury surface impact on 30 April 2015.

The XM2 and XM2′ MESSENGER mission phases provided orbits with mission-unique opportunities for exploring Mercury that required engineering and scientific creativity to extend spacecraft functionality well beyond its design specifications. Significant expansion of the predictive capabilities of spacecraft thermal models and careful coordination of spacecraft pointing were required to extend the spacecraft's eight-year design lifetime to 10.8 years with some late-XM2 orbits that exposed the spacecraft to its most severe thermal conditions of the mission. Having the opposite effect as during the primary and first extended missions, solar gravity perturbations forced the spacecraft's minimum altitude to drift toward Mercury impact. During the final month of flight operations the spacecraft depleted all usable fuel, and then became the first planetary spacecraft to achieve orbit change by intentionally expelling helium pressurant. The final 11 OCMs raised periapsis altitude, thereby delaying Mercury impact and enabling new opportunities for scientific discovery. The mission's final 1.5 months yielded key advances in scientific understanding of Mercury features such as crustal magnetic fields and water ice deposits.

The XM2 mission phase ended in mid-March 2015 with two of the four OCMs having shifted about one day earlier than originally planned. Each XM2 OCM targeted extended periods when periapsis altitude remained near 25 km (after OCMs 9–11) and 15 km (after OCM-12). Completion of OCM-9 ended the mission's longest period, 26 months, between course corrections.

The six-week-long XM2′, MESSENGER's final mission phase, accepted higher operational risk. This elevated risk had to be mitigated twice, as the five-OCM plan became a seven-OCM plan that culminated in Mercury impact with a nearly empty solid-state recorder during the planned final orbit. Extra OCMs were required after adjusting estimates of remaining usable propellant, and after uncertainties in orbit prediction grew during multiple orbits with minimum altitude below 20 km. During XM2′, five of the seven OCMs utilized helium pressurant for orbit change, thereby expanding understanding of the propulsion system capability and also extending science data collection and return by three weeks. Before Mercury impact on 30 April 2015, the XM2′ orbit averaged 15 km in minimum altitude and 8^{h} 17^{m} in orbit period. An important aspect of the XM2′ mission success was the mission design team's close and rapid coordination with the Mission Systems Engineer and the navigation, guidance and control (G&C), propulsion, mission operations, and science teams in order to maximize both mission lifetime and science data return. Other critically important elements of engineering and science coordination that enabled precise prediction of Mercury impact to the orbit periapsis interval planned months earlier was the use of Mercury digital elevation models by laser altimeter scientists and the mission design team for maneuver design and post-maneuver evaluation, along with meticulous attention to detail via the orbit determination process by the navigation team[4].

SECOND EXTENDED MISSION – DESCENDING TOWARD MERCURY

Periapsis Progression and Maneuver Placement

MESSENGER's second extended mission effectively utilized most of the remaining propellant by implementing spacecraft pointing strategies that preserved spacecraft function amidst new highs of spacecraft bus heating. Figure 1 shows altitude and sub-spacecraft Mercury latitude at periapsis, as well as "hot seasons" (i.e., when periapsis was near the sub-solar longitude during the noon-midnight orbit configuration) and a late-mission superior solar conjunction. Four OCMs at apoapsis during the dawn–dusk orbit each increased periapsis altitude sufficiently to target periapsis altitudes of 25 km (three times) or 15 km (once). Each MESSENGER OCM was constrained to execute only with the spacecraft's sunshade protecting the spacecraft bus from direct sunlight. The size of the periapsis altitude increase required a ΔV that was most efficiently imparted by the largest monopropellant thrusters near dawn–dusk orbits, because periapsis altitude changed little over several consecutive orbits at such times. The dawn–dusk orbit option for OCM-12 was postponed from the December 2014 solar conjunction to the next best time for OCMs on 21 January 2015 to avoid solar interference disrupting communication when the Sun-Earth-probe (SEP) angle was < 3°. Times when solar incidence angle is > 84° in Figure 1 correspond to intervals when periapsis was either near or over shadowed portions of Mercury's surface. The portions of the curves in red in Figure 1 indicate times when poor lighting prevented imaging at or near periapsis. A horizontal dashed line marks 25-km periapsis altitude, the target for OCMs 9−11.

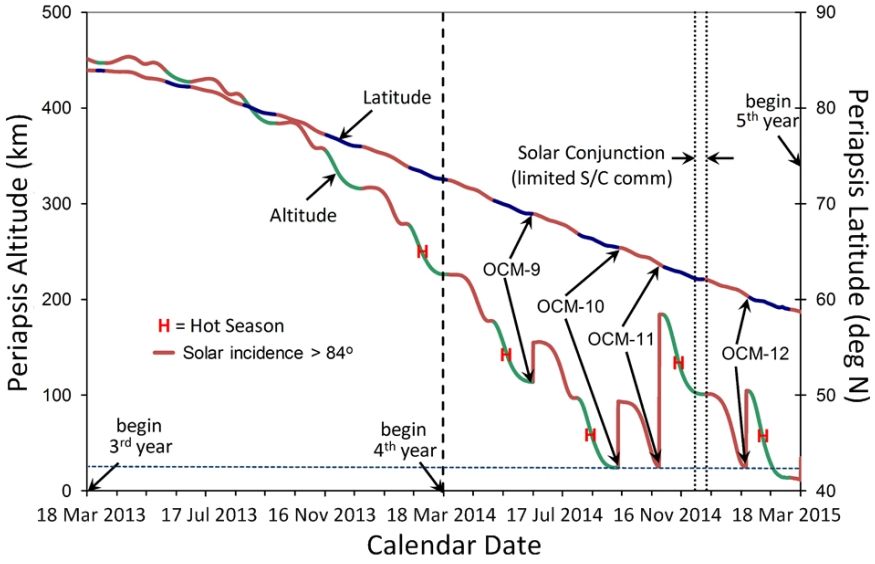

Figure 1. Periapsis Evolution during MESSENGER's Second Extended Mission.

Maneuver Implementation and Results

The four OCMs of XM2 included the final two OCMs that used propellant from one of the two main fuel tanks, as well as two OCMs that utilized propellant only from the small auxiliary fuel tank. The propulsion subsystem layout including thruster orientations and thruster set velocity change directions are depicted in Figure 2. Detailed coverage of the implementation of OCMs 9−11 was provided previously[5]. An update of tabular information from a paper[3] that outlined plans for OCMs 9−12 is in Table 1. Sun elevation angle in Table 1 equals Sun-S/C-ΔV angle minus 90°. Although the objectives of these four OCMs did not change, the actual performance of OCMs 9−12 affected plans for the six-week XM2′ extension of XM2.

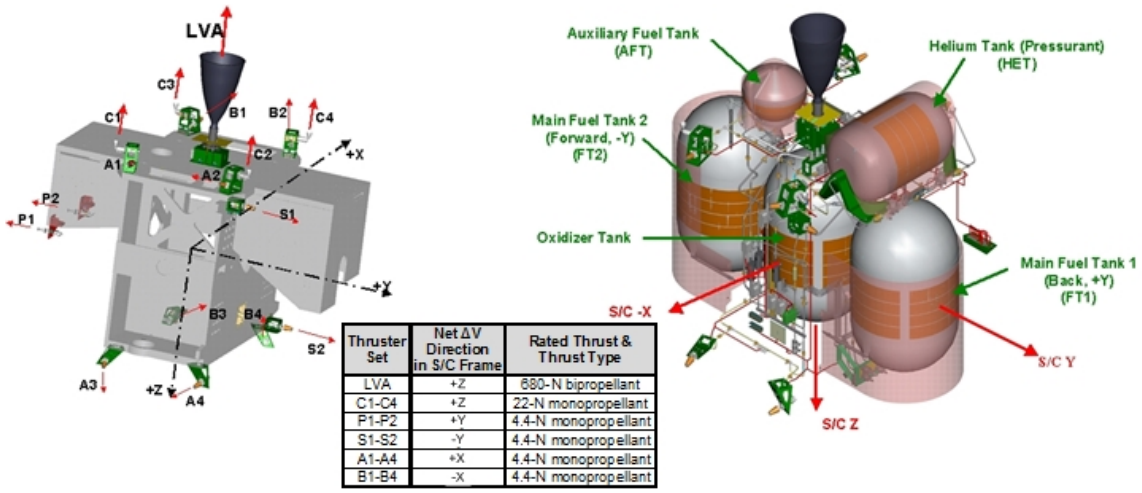

Thruster Set	Net ΔV Direction in S/C Frame	Rated Thrust & Thrust Type
LVA	+Z	680-N bipropellant
C1-C4	+Z	22-N monopropellant
P1-P2	+Y	4.4-N monopropellant
S1-S2	-Y	4.4-N monopropellant
A1-A4	+X	4.4-N monopropellant
B1-B4	-X	4.4-N monopropellant

Figure 2. MESSENGER Propulsion System with Tanks, Thrusters, and Spacecraft Coordinate Axes. S/C = Spacecraft.

Table 1. Summary of Maneuvers during Mercury Orbital Phase XM2.

Maneuver and Result	Prime Thrusters-Segment Name	Calendar Date (day month year)	Start UTC (hh:mm:ss)	Sun Elevation (°)	Duration (s)	ΔV (m/s)
OCM-9 raised periapsis to attain a minimum altitude of 24.2 km prior to OCM-10.	A1A2B1B2-settle	17 Jun 2014	14:53:00	5.62	60.0	0.421
	C1C4 - main	17 Jun 2014	14:54:00	----	54.0	4.158
	A1A2B1B2 - trim	17 Jun 2014	14:54:54	----	76.0	0.440
	Post-OCM-9 usable fuel = 10.211 kg (1.873 kg used)			**OCM-9 total ΔV = 5.020 m/s**		
OCM-10 raised periapsis to attain a minimum altitude of 25.6 km prior to OCM-11.	A1A2B1B2-settle	12 Sep 2014	15:54:29	4.47	59.0	0.328
	C1C4 - settle	12 Sep 2014	15:55:28	-----	36.0	2.288
	C1toC4-main/trim	12 Sep 2014	15:56:04	-----	39.1	5.943
	Post-OCM-10 usable fuel = 7.976 kg (2.161 kg used)			**OCM-10 total ΔV = 8.554 m/s**		
OCM-11 raised periapsis to attain a minimum altitude of 25.2 km prior to OCM-12.	C1toC4-main	24 Oct 2014	18:58:12	3.00	149.9	19.341
	+0.807 kg usable fuel adjustment after OCM-10 evaluation **Post-OCM-11 usable fuel = 4.138 kg (4.600 kg used)** **OCM-11 total ΔV = 19.208 m/s**					
OCM-12 raised periapsis to attain a minimum altitude of 14.8 km on 1 Mar 2015.	C1toC4-main	21 Jan 2015	18:27:24	-4.14	109.1	9.633
	+0.314 kg usable fuel adjustment after OCM-11 evaluation **Post-OCM-12 usable fuel = 1.823 kg (2.296 kg used)** **OCM-12 total ΔV = 9.744 m/s** **-0.253 kg usable fuel adjustment after OCM-12 evaluation**					

As the spacecraft's usable propellant neared depletion in each main fuel tank, propellant management procedures prevented usable fuel from migrating and becoming trapped above the main fuel tank baffles. For example, OCM-9 began with a fuel-settle segment that used four 4.4-N A/B thrusters, continued with a main segment with two 22-N C-thrusters imparting 83% of the OCM-9 total ΔV, and concluded with a trim segment that used four 4.4-N A/B thrusters. The auxiliary fuel tank supplied fuel for OCM-9. Although most MESSENGER OCMs ended with a short "tweak" segment that used almost no fuel and imparted close to zero ΔV, the tweak segments are not listed here. The apoapsis-centered OCM-9 raised the spacecraft's terrain-relative minimum altitude from 115.0 km to 156.4 km, which ensured that the orbiter came no closer than

24.2 km (25 km target) above Mercury's surface when periapsis altitude changed little for many consecutive orbits just before OCM-10 on 12 September 2014. The spacecraft's orbit period increased by 1.9 minutes, from 8h 0m 9s to 8h 2m 2s, during OCM-9. The mission design team targeted XM2 and XM2' OCMs using terrain-based minimum altitudes based on a northern-hemisphere digital elevation model supplied by the MESSENGER science team and derived from Mercury Laser Altimeter (MLA) instrument observations. Figure 3 illustrates the difference between terrain-based altitude and altitude relative to a 2440-km-radius reference sphere from the OCM-11 final design. Specific ΔV performance for all OCMs was reported by Moessner and McAdams[6].

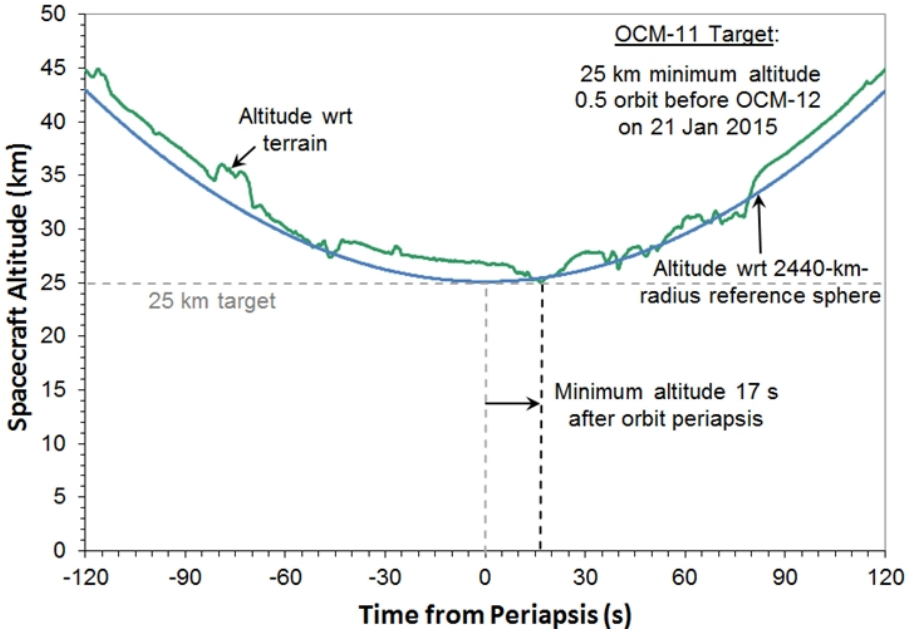

Figure 3. Altitude Variation due to Topography from a Mercury Digital Elevation Model.

The next raise in periapsis altitude came from OCM-10, the last MESSENGER maneuver to rely on usable fuel from either of the main fuel tanks. About one Mercury year after OCM-9, the apoapsis-centered OCM-10 increased the terrain-relative minimum altitude from 24.2 km to 93.5 km and achieved a minimum terrain-relative altitude of 25.6 km about one-half Mercury year later, when periapsis altitude reached a local minimum about 1.5 orbits before OCM-11. In order to consume nearly all accessible fuel contained in the only main fuel tank with usable fuel remaining, a multi-segment design was needed. Two fuel-settle segments using fuel from the auxiliary fuel tank (AUX) were conducted. The first fuel segment used four A/B thrusters, and the second settle segment used two C-thrusters. A 22-s duration main-segment burn with four C-thrusters then depleted usable fuel from main fuel tank 2. Since fuel in fuel tank 2 (FT2) depleted 22 s into the 30-s segment, the final 8 s relied on helium gas pressurant from FT2. Then a 9-s trim segment using four C-thrusters with fuel from the auxiliary fuel tank completed OCM-10.

The next apoapsis-centered maneuver, OCM-11, raised the spacecraft's terrain-relative minimum altitude from 25.6 km to 184.6 km and achieved a terrain-relative minimum 25.2-km altitude about one Mercury year later, when periapsis altitude reached a local minimum about 1.5 orbits before OCM-12. With no need to conserve usable fuel in the main fuel tanks, OCM-11 was performed using a single four-C-thruster segment that drew fuel only from the auxiliary fuel tank.

The final XM2 maneuver, OCM-12, raised the spacecraft's terrain-relative minimum altitude from 25.2 km to 105.1 km in order to attain a local minimum of 14.8 km above Mercury's terrain on 1 March 2015 – during the final period before Mercury impact within which periapsis altitude varied by less than 2 km over 1.5 weeks. Emptying both FT1 and FT2 of usable fuel, OCM-12 occurred at apoapsis and used one four-C-thruster segment drawing fuel from the auxiliary fuel tank. After a post-OCM-12 check of pressure in the auxiliary fuel tank, the estimate of usable fuel remaining in the auxiliary tank was changed to about 1.82 kg. Without additional OCMs, MESSENGER flight operations would have ended with a 28 March 2015 Mercury impact.

LOW-ALTITUDE HOVER CAMPAIGN – CONDUCTING SCIENCE UNTIL THE END

With less than 0.3% remaining of the 591 kg of usable propellant and about 95% of the 2.3 kg of helium pressurant at the time of launch 10.7 years earlier (a total of 599.4 kg of loaded propellant and pressurant[7]), the team embarked on a high-reward, moderate risk, final 0.12-year mission extension. Having measured a small amount of ΔV during the expulsion of helium gas pressurant during OCM-10 and OCM-12, engineers were optimistic that recently identified, mission-unique XM2′ science objectives could be attained with prudent use of the remaining usable hydrazine fuel and helium pressurant. The science team obtained permission to operate the spacecraft in ways never envisioned by the spacecraft designers by using frequent OCMs to limit minimum altitude variation to less than 30 km between OCMs and to allow minimum altitudes as low as 7 km prior to the final descent to impact. This narrow range of periapsis altitudes led to the term "hover" campaign for XM2′. Accomplishing this demanding objective required using frequent OCMs during a time of substantial uncertainty in the usable propellant remaining, from Sun-relative orbit orientations much different from those for any of the previous 12 OCMs, as well as other challenges discussed below. Before exploring the XM2′ engineering challenges and how they were overcome, it is important to understand key the science rationale and science results that justified the increased risk during the final weeks of MESSENGER flight operations.

XM2 Prime Science Rationale and Results

Between insertion into orbit about Mercury on 18 March 2011 and impact onto the planetary surface on 30 April 2015, MESSENGER collected an extensive set of measurements of Mercury and its space environment suited to answer the specific scientific questions that framed the primary and extended mission phases. One science objective was to determine the nature and origin of Mercury's internal magnetic field, which was discovered during two flybys of the innermost planet by Mariner 10 in 1974 and 1975. The Mariner 10 observations provided only an approximate estimate of the planetary dipole moment, because of limited spatial sampling and contributions to the measurements from magnetic fields arising from sources external to the planet. Observations by MESSENGER of the magnetic field during four Earth years (more than 16 Mercury years) enabled detailed characterization of Mercury's internal[8] and external[9,10] magnetic fields. Analyses of these observations showed that Mercury's dipole field is closely aligned with the planet's spin axis, is offset by 480 km northward along the spin axis, and has a moment of 190 nT R_M^3, where R_M=2440 km is Mercury's radius[7].

Small-wavelength structures in the field originating from higher-order core fields and/or crustal magnetization could not be measured during the primary mission because the signal from these contributions at periapsis altitudes of 200−500 km proved to be too weak and were often overwhelmed by large variations in the external magnetic field. The first definitive observations of small-scale magnetic fields associated with crustal magnetization were obtained during XM2 at spacecraft altitudes below 70 km, where the signal is larger because of the smaller distance between the observation point and the magnetization source[11]. Figure 4 shows radial magnetic anomalies with amplitudes of several nanoTeslas (nT) over the Suisei Planitia region. The

underlying image in Figure 4 shows the smooth plains in dark gray and intercrater plains in light gray. The anomalies are coherent between consecutive orbits and between traversals of the region in successive Mercury years and scale inversely with the cubed distance from the source (higher amplitudes associated with lower spacecraft altitudes). From these observations a source depth of up to a few tens of kilometers was inferred, suggesting magnetized crustal rocks as the source of the observed fields rather than contributions from the core.

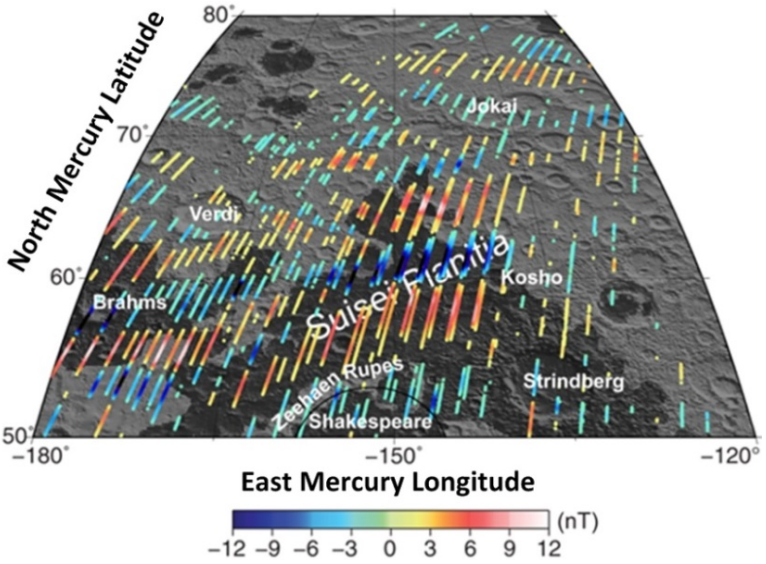

Figure 4. Radial Magnetic Field Anomalies Observed during Orbits 3411–3433 (September 2014) and Orbits 3928–3940 (March 2015) at Altitudes of 25−60 km and 14−40 km, respectively[11].

Observations obtained during XM2 have firmly established the presence of crustal magnetic anomalies and extended the known temporal baseline of Mercury's internal magnetic field by eight orders of magnitude (from 40 years to 4 billion years). However, crustal magnetic anomalies had thus far been detected over only two regions, possibly because the associated signals were below the detection limit at their sampled altitudes over other areas. To establish the distribution of crustal magnetic anomalies on Mercury, one must measure short-wavelength magnetic fields at low altitude over a larger area and ascertain which of those magnetic field variations can be attributed to crustal magnetic anomalies. Acquisition and analysis of these data should provide new information on the mineralogy of Mercury's crustal materials and were the primary motivation for the low-altitude hover campaign executed during XM2′.

Other research areas also benefited from low-altitude observations. Imaging observations revealed the morphology of frozen volatiles in Mercury's permanently shadowed polar craters[12], and MESSENGER's Neutron Spectrometer documented hydrogen-rich material within the polar deposits[13]. Measurements of neutron flux over individual polar deposits in permanently shadowed impact craters at low altitude during XM2′ may have provided the first spatially resolved measurements of excess hydrogen in candidate water-ice deposits within high-latitude craters. Moreover, there is evidence that plasma precipitates from the magnetosphere to the surface and that this process sputters material from the surface in return[14]. Spacecraft attitude during XM2′ periapsis passes was suitable for the Fast Imaging Plasma Spectrometer to observe precipitating as well as upwelling ions. Finally, the lower spacecraft altitude during XM2′ enabled laser ranging observations south of the planetary equator. Together with additional Doppler observations by the radio science experiment, these observations are expected to improve models for Mercury's shape and gravity field.

Maneuver Strategy and Results

More than 12 factors affected the number and placement of OCMs during XM2′. These OCM strategic factors originated from mission design constraints, propulsion subsystem performance, science objectives, or mission operations constraints. Several iterations of the XM2′ maneuver plan, trajectory design, and Mercury impact timing were necessary to include improvements in OCM optimization, as well as late-breaking developments in propulsion performance and science plans. In order to conduct five to seven OCMs within six weeks, the OCM design-to-implementation process was streamlined. The accuracy of OCMs 15−18 was poorer than for earlier maneuvers, but not as a result of this streamlined design and test process. Factors that affected OCM performance included uncertainty in the amount of usable fuel, design challenges in using helium pressurant for orbit changes, and needing to use the P thrusters for the first time in over 8.3 years at about 60% closer to the Sun than ever before.

A number of tradeoffs had to be considered in OCM design. The mission design team acquired updates to predicted thruster performance, burn duration limits, science observation opportunities, Deep Space Network (DSN) support tracks, and factors that affected maneuver start time. Some OCM design strategies required enforcing geometric or operational constraints, or maximizing maneuver efficiency for OCMs. For example, a Sun keep-in (SKI) constraint required the net thrust direction to be within 10° of either the spacecraft-Sun direction or 80°–100° from the spacecraft-Sun direction in order to align the ceramic cloth sunshade to shield the spacecraft bus from direct sunlight exposure. With fuel pressure low in the auxiliary fuel tank as usable fuel neared depletion, the most efficient way remaining to impart ΔV would utilize the four C-thrusters to achieve a ΔV in the +*Z* direction. Although OCMs 1−12 were each performed with the orbiter near a dawn–dusk spacecraft orbit when Mercury was near either its aphelion or its perihelion, OCMs 13−18 were all sufficiently far from a dawn–dusk orbit (see Figure 5) that a ΔV penalty resulted from a SKI-compliant thrust direction that was out of the spacecraft's orbit plane.

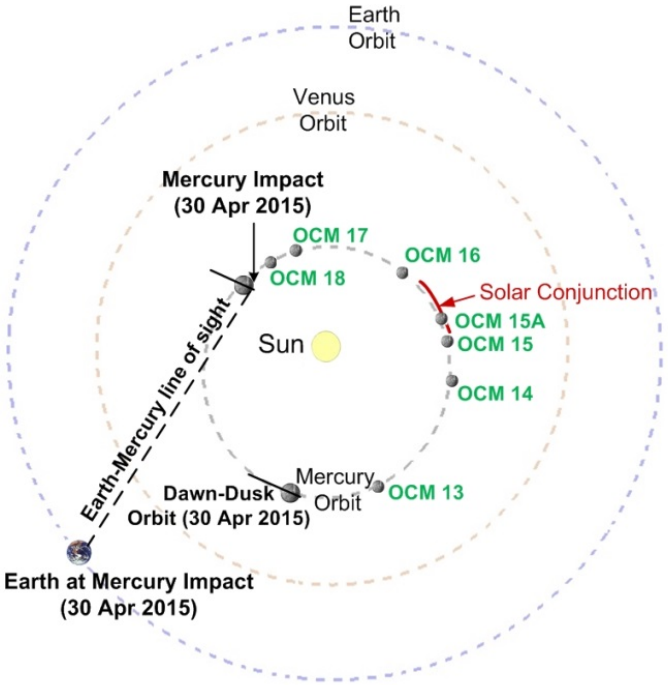

Figure 5. North Ecliptic Pole View of MESSENGER's XM2′ OCM Locations and Line Segments Depicting the Spacecraft Orbit's Line of Nodes.

Instead, these OCMs had to be designed to avoid using the most efficient periapsis-increasing strategy, an apoapsis-centered ΔV that is aligned with the spacecraft's Mercury-centered velocity, and instead used another orbit location and a different thrust vector orientation that maximized the Mercury-relative altitude change per unit propellant mass. With the sub-spacecraft periapsis latitude near 58° N during XM2′ (see Figure 1), and the spacecraft orbit line of nodes > 10° from the dawn–dusk orbit, the optimal OCM start shifted either slightly before or after orbit apoapsis. In addition, all nominal OCMs and three-orbit (~one day) contingency OCMs met the constraint that the SEP angle exceed 3° (i.e., that solar conjunction be avoided).

A quantitative look at propulsive maneuver efficiency for OCM-12 and each subsequent OCM indicates a major difference in maneuver design and implementation for the XM2′ hover campaign. Figure 6 combines all OCM design factors in the context of Mercury's heliocentric orbit location, the time-relative spacing of OCMs, the ratio of periapsis altitude change per propellant used ratio, and where solar conjunction (SEP angle < 3°) degraded or disrupted communication with the spacecraft. The ratio of periapsis altitude change per propellant used is defined as the difference in periapsis altitude after versus before the OCM minus the single-orbit

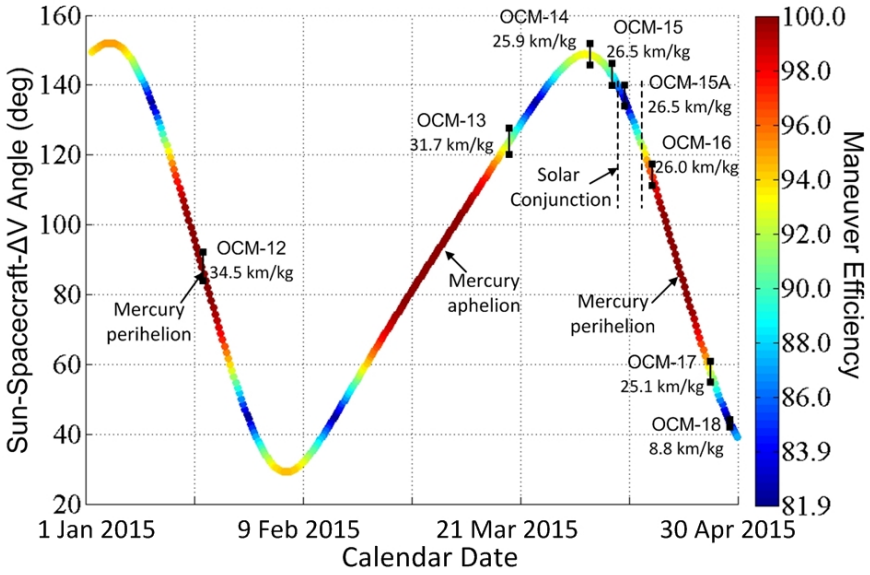

Figure 6. Propulsive Maneuver Efficiency and Periapsis Altitude Change per Kilogram of Propellant Used for Each MESSENGER OCM in 2015.

periapsis altitude change from solar gravity perturbation divided by the mass of fuel (hydrazine) and/or helium gas pressurant expelled from the spacecraft. The vertical axes in Figure 6 are based on a simplified assumption that the velocity change direction aligns with the spacecraft velocity at apoapsis for these periapsis-altitude-raising OCMs. Allowing for a 2° in-OCM variation of the thrust direction, the Sun-spacecraft-ΔV angle must be either between 80° and 100° (Sun elevation angle from −10° to +10°) when using the largest monopropellant C-thrusters or between 170° and 180° when using the sunshade-mounted P-thrusters, as required for OCMs 14 and 15 during a noon–midnight orbit. Maneuver efficiency ranges from 100% to 82%, given by the cosine of 35°, which accounts for the worst-case 45° off-Sun orientation between spacecraft axis-aligned thruster sets, combined with the 10° allowable sunshade tilt. Figure 6 shows maximum maneuver efficiency applying near dawn–dusk orbits (see Figure 5), which occurred near Mercury perihelion and aphelion on 5 March 2015 and 44 days (1/2 Mercury orbit) later during XM2′.

When the orbit was near the noon–midnight orientation, which occurred at OCM-14, the XM2′ 57°–58°N periapsis latitude extrapolated using the trend in Figure 1 and the sunshade SKI constraint led to an optimal maneuver start shifted from apoapsis. The spacecraft's orbit inclination of about 83° during XM2′ also affected the determination of ideal thrust orientation for orbits with orientations near the noon–midnight orientation. The low 8.8 km/kg OCM-18 efficiency was caused by the use of C-thrusters with a ΔV direction more than 70° different from the Mercury-relative spacecraft velocity direction and OCM start time restrictions imposed by the command sequence and scheduled DSN track.

Additional factors affecting the timing of XM2′ OCMs originated from the mission operations, science operations, and propulsion teams. A practice consistent with the previous 12 OCMs was that a second opportunity to complete the ΔV target objective be reserved about one day (three orbits) after the nominal OCM. Although this rule of thumb did not apply to contingency maneuvers OCM-15A or OCM-18, the 1.6-km/orbit decline in minimum altitude above terrain at OCM-14 (see Figure 7) left no more than one orbit margin until Mercury impact after the OCM-15 no-burn (zero ΔV at OCM-15) contingency. Table 2 shows the day of the week

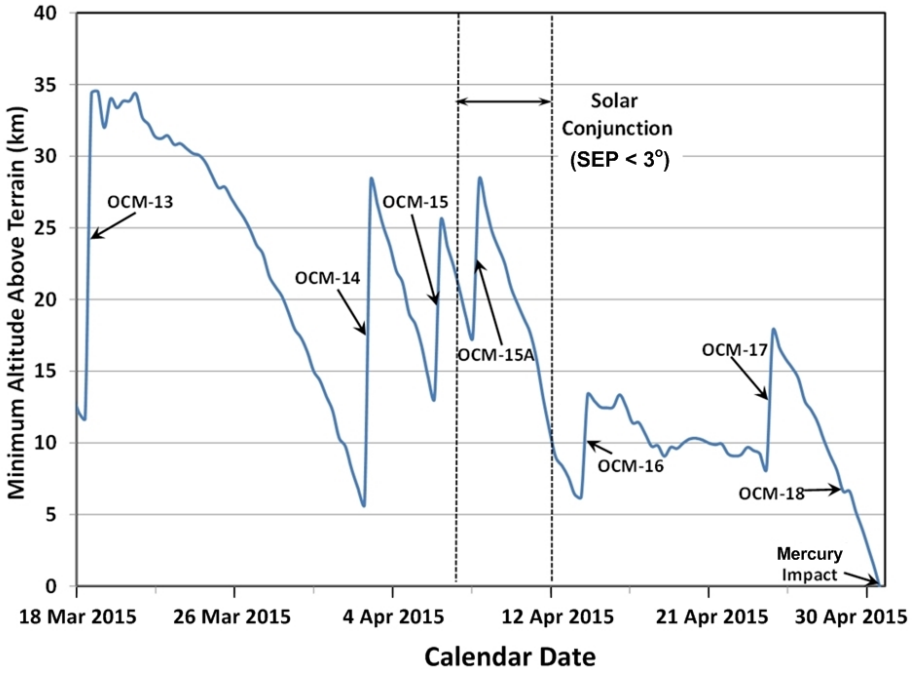

Figure 7. Minimum Altitude Relative to Mercury Surface Topography during XM2′.

and time of day for each OCM, a schedule designed to accommodate a prioritized day-of-week preference for OCMs from the Mission Operations Manager. With Mercury much closer to the Sun than Earth and an orbit period near 8.3 hours, it was not difficult to meet other constraints and schedule OCMs during or close to normal working hours for flight team members in Maryland and Arizona. With a desired minimum altitude before each XM2′ OCM no more than 15 km, and a maximum rate of periapsis decrease near 5 km per three orbits, careful planning was required to keep the closest time between OCMs such that a ΔV underburn might be corrected with an update to the next planned OCM. Another factor that limited the timing of contingency OCMs was the need to fall within scheduled DSN antenna tracks when MESSENGER could be viewed at greater than 20° elevation angle above the local DSN station horizon, and at a time in the planned command load sequence that prevented loss of planned science observations. Science

considerations for OCM timing delayed OCM-13 until minimum altitude descended to just under 12 km and the optimal ΔV direction had not drifted far from the spacecraft velocity direction, indicating minimal loss of propulsive efficiency. A request from the science team delayed OCM-14 from April 1 to April 2 in order to extend high-priority, low-altitude magnetic field observations, thereby increasing signal amplitude by up to a factor of eight over a previously identified region of interest. The final two OCMs before the solar conjunction, OCM-14 and OCM-15, were conducted from spacecraft–Sun-relative orientations near the noon–midnight orbit, which required use of the two small P-thrusters as hydrazine neared depletion. Because helium gas pressurant (GHe) provided only a few percent of the thrust possible when using hydrazine, the GHe OCMs followed the depletion of usable hydrazine when the Sun-relative orbit orientation allowed use of the largest monopropellant thrusters (C1−C4).

Table 2. XM2′ Maneuver Performance from Navigation Team OCM Reconstruction.

OCM #	Start Date, Time (UTC)	Day of Week	Maneuver ΔV		Initial True Anomaly (°)	Sun-S/C-ΔV Angle (°)	SEP Angle (°)	No-OCM Impact Date
			(m/s)	% Error				
13	18 Mar 2015 14:59:39	Wed	3.067	+0.239	178.2	100.0	19.4	28 Mar 2015
14	2 Apr 2015 20:29:44	Thu	3.097	+4.571	184.6	170.0	7.7	4 Apr 2015
15	6 Apr 2015 16:14:07	Mon	1.772	-49.365	187.6	170.0	3.9	10 Apr 2015
15A	8 Apr 2015 16:55:15	Wed	1.833	-4.544	173.5	100.0	1.9	13 Apr 2015
16	14 Apr 2015 15:16:00	Tue	0.957	-2.861	179.9	100.0	5.0	24 Apr 2015
17	24 Apr 2015 17:22:47	Fri	1.492	-2.616	181.4	80.0	15.5	27 Apr 2015
18	28 Apr 2015 21:19:57	Tue	0.425	-3.146	178.3	85.0	18.6	30 Apr 2015

Hydrazine Depletion during OCMs 13 to 15

After observing FT1/FT2 propellant exhaustion during OCM-12, all subsequent maneuvers were limited to drawing propellant from the auxiliary tank, the only tank known to have usable hydrazine. OCMs 13 and 14 were the last two MESSENGER maneuvers, except for momentum desaturations, which executed nominally as hydrazine blowdown burns from the auxiliary tank. OCM-13 raised minimum altitude from 11.7 km to 34.2 km during a 33-s maneuver that used the four MR-106E engines (largest monopropellant thrusters) for primary ΔV and consumed 0.725 kg of N_2H_4 as calculated by the pressure–volume–temperature (PVT) method. OCM-14 raised minimum altitude from 5.4 km to 28.3 km during a 401.2-s maneuver that used the sunshade-piercing P1/P2 thruster pair of MR-111C engines (smallest monopropellant thrusters) for primary ΔV and consumed 0.926 kg of N_2H_4 as calculated by the PVT method. Propellant consumption for both maneuvers tracked well with pre-maneuver predictions, as thruster performance matched established performance curves for the MR-106E and MR-111C.

The introduction of helium into the auxiliary tank during OCMs 10 and 12 had a longer-lasting impact than expected. Thruster performance data suggested that remaining GHe was fully vacated from the auxiliary tank during the final segments of OCMs 10 and 12, as well as during

OCMs 13 and 14, which used more than 1.6 kg of hydrazine from the auxiliary tank without evidence of helium bubbles. The possibility of hydrazine exhaustion prior to OCM-15 was recognized, and the cessation of propellant flow was expected to be abrupt, with the line pressure dropping to the ~1 psi (~7 kPa) vapor pressure of N_2H_4. The Fault Protection subsystem was set to autonomously switch to GHe in FT1/FT2 once the feed pressure dropped below 50 psi (~350 kPa). Instead of a sudden decline, the blowdown and thrust curves in Figure 8 were observed, signifying an unanticipated gradual decline in feed pressure. Thrust magnitude decay tracked with pressure decline well, indicating that propellant flowed continuously to the thrusters prior to the autonomous tank switch. These data suggest that the previously introduced helium remained in the auxiliary tank as a hydrazine froth or foam that was slowly expelled as the diaphragm lowered. This helium masquerading as hydrazine resulted in an overestimation of remaining propellant by about 0.7 kg. Once the latching valves to FT1 and FT2 were opened for the rest of the maneuver, the auxiliary tank was fully pressurized with helium. As the auxiliary tank pressure never again dropped below 90 psi (~620 kPa), hydrazine foam was never observed again.

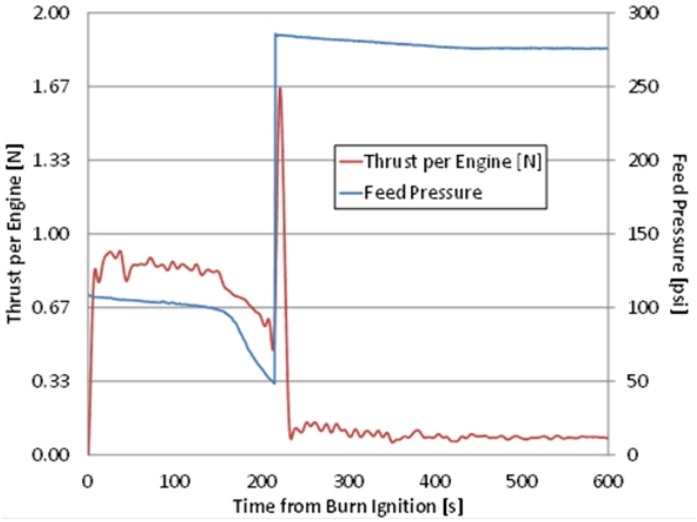

Figure 8. OCM-15 Feed Pressure and Thrust. Gradual Decline Before Autonomous Switch to FT1/FT2 Suggests that Hydrazine was Suffused with Helium Bubbles, Forming a Foam which Slowly Evacuated.

OCM-15, which increased minimum altitude from 13.1 km to 25.4 km, began with a 225-s burn from the P1/P2 thruster pair using N_2H_4 from the auxiliary tank. As shown in Figure 8, seconds 150–214 indicated a gradual decline in pressure and performance consistent with expulsion of frothy hydrazine. The autonomous switch to FT1/FT2 resulted in 11 s of high-feed-pressure (285 psi, or 1.97 MPa) hydrazine flow, presumably from the propellant lines leading to FT1/FT2, though intermittent helium likely prevented the engines from ever reaching nominal steady-state thrust. A subsequent 375 s of cold gas propulsion used pressurant GHe from FT1/FT2 and also pressurized the auxiliary tank. MESSENGER's OCM-15 was the first maneuver by any spacecraft to repurpose pressurant into a primary propellant source. The hydrazine-fueled segment of OCM-15 consumed 0.434 kg of N_2H_4 as calculated by the PVT method. The cold gas segment consumed 0.067 kg of GHe as calculated by the PVT method. Using helium, the 4.4-N nominal MR-111C delivered from an average of 3.3% (OCM-15) to 2.3% (OCM-18) of the equivalent N_2H_4 thrust predicted by Aerojet Rocketdyne's nominal performance curves. Delivered specific impulse, calculated using measured thrust and GHe consumption, was 172 s during OCM-15 and 176 s during each remaining OCM, near the theoretical GHe maximum of 179 s computed by Sutton.[15]

Helium Use during OCMs 15A to 18

The rest of MESSENGER's low-altitude hover campaign was completed using helium propellant regulated at 280 psi (1.93 MPa) maximum from the GHe tank into FT1/FT2 as well as GHe present in the auxiliary tank, since all low-pressure latch valves were permanently opened. All four helium OCMs used the C1/C2/C3/C4 thruster set with four 22-N nominal (5 lbf) MR-106E engines for primary ΔV and the A and B thrusters for attitude control. Prior to OCM-15A the spacecraft had an estimated 1.791 kg (±2%) of usable GHe. After OCM-18 an estimated 0.512 kg of GHe remained, but with 103 psi (710 MPa) feed pressure, further delivered thrust capability was limited.

In order to return the trajectory to the nominal science plan before a communications blackout during solar conjunction, the planning, simulation, uplink, and execution of OCM-15A occurred over an unprecedented two days. OCM-15A, which increased minimum altitude from 17.5 km to 28.4 km, took place on 8 April 2015 at a constraint-violating SEP angle of < 1.9°, and consisted of a 303-s 4C cold gas "burn" off of FT1, FT2, and the auxiliary tank. OCM-15A consumed 0.494 kg of GHe as calculated by the PVT method.

OCM-16 and OCM-17, both in the nominal XM2′ plan, were performed as cold gas "burns" off of FT1, FT2 and the auxiliary tank. The 203-s duration OCM-16, which increased minimum altitude from 6.5 km to 13.1 km, took place on 14 April 2015. OCM-16 consumed 0.294 kg of GHe as calculated by the PVT method. The 469.2-s duration OCM-17, which increased minimum altitude from 8.3 km to 18.1 km, took place on 24 April 2015. OCM-17 was followed by a 314-s "tweak" maneuver[16] for attitude maintenance using the A/B thrusters. With the tweak engine duty cycles being about 0.01%, effectively zero propellant was used. OCM-17 consumed 0.434 kg of GHe as calculated by the PVT method.

An underestimation of the trajectory alteration, the result of Mercury's gravity field variations at low minimum altitude, resulted in a nominally completed OCM-17 that would have led to Mercury impact one orbit earlier than planned, a situation that would have prevented downlink of a substantial amount of data on the spacecraft's solid-state recorder during a high-data-rate 70-m DSN antenna track early on 30 April 2015. OCM-18, which increased the minimum altitude from 5.4 km to 6.5 km, took place on 28 April 2015 and consisted of a 303-s 4C cold gas "burn" off of FT1, FT2, and the auxiliary tank. The 1.05-km propulsive portion of minimum altitude change was less than the 1.46-km decrease in periapsis altitude induced by solar gravity between the periapses before and after OCM-18. Consuming 0.114 kg of GHe as calculated by the PVT method, OCM-18 returned the spacecraft's Mercury impact to the desired orbit.

G&C Team Strategy for Maneuver Implementation and Results

Without changes to implementation methods, the commands that executed the quick succession of hover campaign maneuvers would have been nearly impossible to plan, simulate, test, build, and upload to the spacecraft within the allotted time. To reduce the team workload, engineers developed a series of maneuver-enabling macros that used a set of changeable parameters to enable faster build, test, and upload cycles. The hover macro reduced the number of detailed reviews required without increasing risk, but also added constraints that limited maneuver design flexibility. Prior to implementing the hover macro, the attitude control deadbands used by the G&C software were chosen to optimize burn performance for each maneuver type. During XM2′, limitations on macro space required the attitude control deadbands to provide acceptable limits for all maneuver and commanded momentum dump configurations. The single set of parameters also had to provide acceptable performance across varying thrust scenarios of hydrazine, gas, or a combination of the two. Creating a default set of universal thruster control parameters introduced slightly more pointing error than was seen previously, but

was still within the tolerance of the hover campaign maneuver execution requirements. Typical maneuvers had pointing errors <1°, whereas the hover OCMs were expected to have pointing errors up to approximately 4°. Pointing errors and other details of the hover campaign maneuvers appear in Table 3. Comparing final ΔV magnitude errors in Table 2 with preliminary accelerometer-based ΔV magnitude errors in Table 3 reveals close agreement within 0.2% (typical of orbital-phase OCMs) for OCM-13, and agreement within 3%−5% during the P-thruster and GHe-propellant OCMs 14-18. The updated parameters were also chosen to reduce the on time of the 4.4-N A- and B-thrusters, which are about 74% less efficient for imparting ΔV than the 22-N C-thrusters. Forcing the control system to maintain attitude control primarily with the C-thrusters contributed to additional minor propellant savings.

Table 3. XM2′ Maneuver Summary from Guidance and Control Team OCM Estimates.

OCM #	Calendar Date (day month year)	Main Thrusters	Fuel Source	Duration (s)	ΔV Magnitude Error** (%)	Burn Pointing Error** (°)	Average Thruster Duty Cycles	
							Attitude Control§	Main ΔV
13	18 Mar 2015	22-N C1-C4	N_2H_4	32.96	0.412	0.627	0.38 %	99.5 %
14	2 Apr 2015	4.4-N P1-P2	N_2H_4	401.24	-0.015	3.978	18.76 % A2,A4,B2,B4	96.3 %
15	6 Apr 2015	4.4-N P1-P2	N_2H_4 and GHe	600.00*	-50.67	2.760	11.53 % A2,A4,B2,B4	94.6 %
15A	8 Apr 2015	22-N C1-C4	GHe	303.00*	-0.132	1.248	0.26 %	97.8 %
16	14 Apr 2015	22-N C1-C4	GHe	201.92	0.020	0.695	0.08 %	99.5 %
17	24 Apr 2015	22-N C1-C4	GHe	469.22	0.167	0.751	0.06 %	98.9 %
18	28 Apr 2015	22-N C1-C4	GHe	181.02	0.176	1.295	0.00 %	96.2 %

* OCM-15 and OCM-15A terminated due to a maximum burn duration timeout.
**Errors estimated by ground processing of inertial measurement unit (IMU) accelerometer data.
§ C-thruster burn attitude control thrusters are A1-A4 and B1-B4 fired in coupled pairs.

The average attitude-control thruster duty cycles in the hover OCMs were lower than for most previous maneuvers, signifying that the primary ΔV-imparting thrusters were opening and closing more often to control spacecraft attitude and compensate for different levels of thrust from the active thrusters. Attitude control and main thruster duty cycles are shown in the last two columns of Table 3. Except for OCM-15, all XM2′ maneuvers were within expected ranges of both pointing and magnitude error, despite the less than expected thrust produced by the helium. Large maximum-burn-duration timeout values enabled thrusting to continue well past the designed duration until the desired ΔV or timeout was reached.

Maneuver Scheduling and Real-Time Monitoring

In order to support the XM2′ maneuvers, the mission operations team worked closely with the mission design team to define the placement of OCMs 13−18. During the four years and 12 OCMs before XM2′, mission planners defined OCM dates months before execution so that DSN coverage was obtained to support the optimal maneuver placement. For XM2′, however, several concurrent factors were considered sometimes only weeks before the OCM rather than months before. Although most DSN tracks were set months in advance, they were scheduled with the hover campaign in mind, thereby providing a range of selection options. The resulting availability of well-placed DSN tracks was fortunate because of late changes in the number of maneuvers,

refined estimates of available liquid propellant, and changes to the minimum altitude the team was willing to descend to before final descent to impact. DSN coverage of OCMs ultimately worked out well, but both the mission operations and mission design teams accepted compromises by accepting either non-optimal OCM placement or non-optimal real-time coverage in the command sequence. DSN track coverage was intentionally sparse during XM2′ in order to focus spacecraft pointing on the crucial low-altitude science data acquisition rather than Earth-pointing opportunities. The flight team did not have to conduct any maneuver outside of a DSN contact without monitoring the carrier signal and Doppler residuals, which would have been needed only for contingency OCM clean-up to avoid early impact. Another contributing factor specific to OCMs 15 and 16 was reliable commanding opportunities near the superior solar conjunction from 7 to 12 April 2015. When solar elongation is less than 3°, commands can be dropped and telemetry downlink can drop out, so those OCMs were not optimally placed. Lastly, OCMs 15A and 18 were quickly planned clean-up maneuvers. With multiple contingency opportunities for each OCM, the team decided which track to target for these OCMs on the basis of confidence in minimum altitude predicted, sufficient time for testing, and uplink opportunities.

Engineering Challenges of the Hover Campaign

There were numerous challenges the team had to overcome to successfully execute the hover campaign and to ensure completion of the XM2′ science objectives. Several of these challenges (vehicle thermal safety, science planning and data prioritization, communications and orbit determination during solar conjunction) were managed successfully during the orbital mission, but management procedures were modified in response to circumstances unique to the hover campaign. Many other challenges (modified risk posture, heightened cadence of operations, limited contingency response time, streamlined maneuver implementation, use of GHe as a propellant, and managing an uncertain propellant budget) were new to the team, and these circumstances required new approaches to management and mitigation.

Perhaps the most substantial challenge to orbital operations was ensuring the spacecraft's thermal safety. Surprisingly, this challenge was not a major design or implementation issue for the hover campaign. Infrared (IR) heating from Mercury drove the spacecraft's thermal response given that the sunshade managed direct solar heating effectively, and the hover campaign placed the vehicle nominally closer to the IR source. However, the bulk of the hover campaign occurred while the spacecraft was in or near a dawn–dusk orbit (when the orbit ground-track is near the day–night terminator), and heating in this season was consistent with prior Mercury orbital phase experience. The thermal challenges were far greater during noon–midnight orbit seasons. Fortunately, the hover campaign plan forecasted the orbiter to be out of propellant near the beginning of a noon–midnight season that would have led to potentially unmanageable heating. These expected thermal conditions helped solidify the 30 April 2015 Mercury impact target date.

Managing the science activities during the hover campaign followed an approach similar to that used throughout the earlier portions of the mission orbital phase. Two key changes were made to the science planning approach that reduced mission operations workload and made the plan robust with respect to deviations from the planned periapsis altitude profile. First, the science team prioritized data collection campaigns, and the operations team used these priorities to restructure the file downlink priorities so that no manual adjustment of instrument files was necessary. The second change involved blocking out a period of up to several hours around periapsis where spacecraft attitude was defined much earlier. This step was possible because the low-altitude periods did not require targeted observations, and the science priorities during these periods were driven by the non-directed instruments (notably the Magnetometer). This procedure allowed the attitude plan to be robust with respect to failed or partially successful burns (and the attendant orbit period differences). This second change greatly reduced the testing and analysis

burden on science planners, the guidance and control team, and the operations team, without risking science objectives or vehicle safety.

The hover campaign carried substantial additional risk beyond that managed by the team through the earlier portions of the orbital phase, mostly due to the continued risk of untimely surface impact and the resulting cadence of maneuvers necessary to keep the periapsis altitude in the desired corridor. The MESSENGER team worked throughout orbital operations to establish a process for planning and collecting science observations and ensuring vehicle safety. During the hover campaign, the existing team managed the additional risk as well as planned, designed, and executed the series of maneuvers. To streamline the process, less rigor was applied to several elements of vehicle operations. Reviews were consolidated and conducted as less formal peer reviews. Rather than designing and testing contingency maneuvers for each scheduled maneuver (as was typical throughout the earlier phases of the mission), the team worked on a plan that would allow any such contingency maneuver to be rapidly designed and implemented. This strategy worked well, helping to reduce workload, and did not compromise the ability of the team to design and execute two contingencies needed during the hover campaign (following a ~50% underburn due to untimely hydrazine depletion and an unplanned maneuver that delayed surface impact by one orbit).

One of the biggest challenges of the hover campaign was working within the propellant budget uncertainty. First, the amount of accessible hydrazine was not well known. Second, the performance of GHe when used as a propellant was uncharacterized when planning XM2′. At the time of planning the hover campaign, an approach identified a mission end date that appeared achievable with conservative assumptions about the thrust and specific impulse from the GHe. A carefully developed maneuver sequence allowed full depletion of the onboard hydrazine before relying on GHe for OCMs. This choice helped to increase confidence that at least a portion of the hover campaign was achievable, even if the GHe proved ineffective or caused problems for the health of the propulsion system (latch and thruster valve overheating were particular concerns). Ultimately, the hydrazine was depleted earlier than expected, before OCM-15 ran to completion. Despite the early hydrazine depletion, careful fault management allowed autonomous transition to GHe usage, and the subsequent maneuvers (OCMs 15A, 16−18) were executed solely with GHe, successfully achieving the desired Mercury impact epoch.

The first-ever navigation of a spacecraft at Mercury periapsis altitudes well below 25 km led to special challenges. These challenges included improving the Mercury gravity field model, observation modeling during superior solar conjunction, and radiation pressure modeling. At these lower altitudes, force models for the Mercury gravity field and the thermal radiation emanating from the hot surface of the planet had not been characterized beyond what had been observed at higher altitudes.

On the basis of an *a priori* Mercury gravity field model determined between MOI and well into the mission orbital phase, the navigation team supported weekly orbit solutions by providing estimates of minor variations in gravity field coefficients, estimates that had to be tightly constrained by appropriate uncertainties in each coefficient. Leading up to the low-altitude hover campaign when the periapsis altitude of the spacecraft was well below 200 km, the navigation team began using a hybrid approach to gravity modeling and estimation. This entailed incorporating higher-order terms from the HGM006 field (no corresponding publication as of early August 2015) produced by the MESSENGER science team, complete to spherical harmonic degree and order 75, while estimating the first 20×20 field coefficients on the basis of the graduated scaling of *a priori* values and uncertainties.

The navigation team typically defines entry of superior solar conjunction to be when the Sun-Earth-probe angle drops below 10°, where radiometric signals can be degraded measurably as they pass through the solar plasma. A superior solar conjunction occurred during the low-altitude hover campaign, which encompassed most of the final OCMs. During this conjunction, Doppler data weights had to be manually adjusted by observed noise level for each tracking pass.

Specular and diffuse reflectivity coefficients and overall scale factors for solar radiation pressure (SRP), planetary (infrared) radiation pressure (PRP), and planetary albedo were estimated filter parameters. The infrared model was based on a spherical harmonic representation of a model of sub-solar temperature distribution[17]. During the initial stages of the hover campaign, the orbit determination (OD) filter occasionally produced physically unrealistic values for PRP coefficients and scale factors (e.g., negative values), indicating limitations in model fidelity and possible aliasing between estimated model parameters. However, as experience was gained at low altitude and estimation strategies were refined, estimated radiation parameters were generally well behaved. Although some adjustment of the estimated parameters associated with those models could be accommodated by the OD filter when flying at lower altitudes during periapsis passages, there was the potential for large uncertainties in the future behavior of the spacecraft orbit during the longer (5 week) propagation spans that often occurred at much different altitudes than during the (3–7-day-long) fit span.

ORBIT DETERMINATION AND MANEUVER RECONSTRUCTION

Overview of Navigation Operations

Throughout the MESSENGER mission, the KinetX Aerospace navigation team was responsible for processing NASA DSN radiometric tracking data to produce the current and projected best estimate of the spacecraft trajectory for use in mission operations, science observation planning, and DSN tracking. In addition, the navigation team worked closely with the mission design team at JHU/APL to validate and model orbit correction maneuvers. KinetX used the MIRAGE suite of software tools to perform high-precision orbit estimation and maneuver design validation for the MESSENGER spacecraft.

During the MESSENGER mission, fine tuning of various parameters[4] helped to improve the accuracy of orbit determination and prediction for both the mission design and navigation teams. Table 4 summarizes the model parameters used by the navigation team during the MESSENGER orbital operations phase. Estimated parameters were explicitly determined as part of the solution for the spacecraft "state vector." "Consider" parameters were only used in the determination of formal uncertainties associated with estimated parameters.

Table 4. Summary of Model Parameters for OD Solutions.

Estimated Parameters	Consider Parameters
Position and velocity Solar and planetary radiation pressure specular and diffuse reflectivities Mercury albedo specular and diffuse reflectivities ΔV due to commanded momentum desaturations Orbit-correction maneuvers Mercury ephemeris Mercury gravity field (20×20 spherical harmonic expansion)	Station locations Troposphere model parameters Ionosphere model parameters Earth pole, UT1 Earth ephemeris

Use of Laser Altimeter Data to Monitor Periapsis Altitude Estimates

Daily data from the Mercury Laser Altimeter (MLA) were utilized as a cross-check on the estimates of periapsis altitude reconstructed and predicted by the navigation team during the hover campaign. Figure 9 shows an example of information produced by the MLA team for a

single periapsis passage in order to assist the navigation team in their assessments of the accuracy of periapsis altitude predictions. Such data proved invaluable in evaluating alternative estimation strategies, including adjustments to Doppler data weights and shortening of fit spans, and eventually allowed the navigation team to settle on a strategy that gave consistently accurate predictions. MLA data, which were obtained on a daily basis between OD deliveries, confirmed that the propagations were sufficiently accurate to support maneuver design and observational planning, and ultimately to confidently predict the time and location of impact onto Mercury about one week before impact.

Reconstruction of Hover Campaign OCMs by the Navigation Team

Another challenging aspect of XM2′ was the need to rapidly determine OCM performance. Reconstruction of an OCM was often required within 24 hours of execution to meet operational constraints. Reconstruction was aided by post-OCM estimates of burn start time, duration, and achieved ΔV provided by the guidance and control team on the basis of downlinked accelerometer data. This situation was particularly useful for OCM-15, which underperformed by about 50% due to the depletion of all hydrazine mid-burn, and the resulting changeover to gaseous helium propellant. The navigation team was able to rapidly reconstruct OCM-15 and provide an updated trajectory to the mission design team to turn around a clean-up OCM (OCM-15A) within 48 hours of OCM-15. Table 2 summarizes the final OCM ΔV reconstruction.

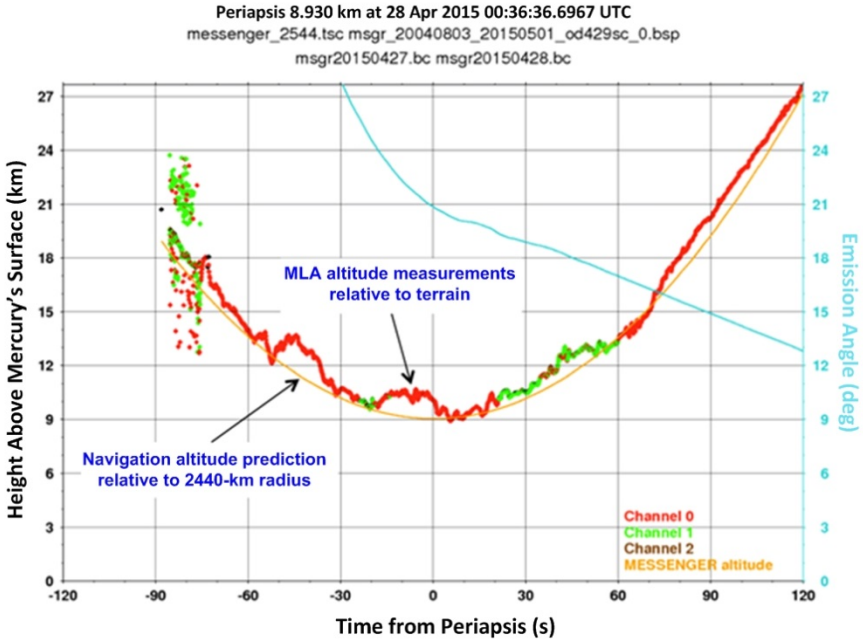

Figure 9. MLA-based Periapsis Altitude Profile Compared with the Profile Predicted by the Navigation Team (Courtesy of Gregory A. Neumann and Erwan Mazarico)

TARGETING MERCURY IMPACT

About seven weeks before the start of the low-altitude hover campaign, at a 28 January 2015 XM2′ kickoff meeting, the flight team received details of a seven-OCM sequence that ended in Mercury impact on 30 April 2015 at about 19:25 UTC. Although implementation details and OCM times changed during the next three months, the orbiter completed seven OCMs and impacted Mercury at about 3.912 km/s on 30 April 19:26:01.166 UTC at 54.440° N latitude and 210.120° E longitude. Figure 10 shows a view from Earth at that time with the lower left of the

letter “M” in MESSENGER representing the Mercury-occulted impact location, as well as a view of the final portion of the trajectory over Mercury with a marker showing the Mercury impact.

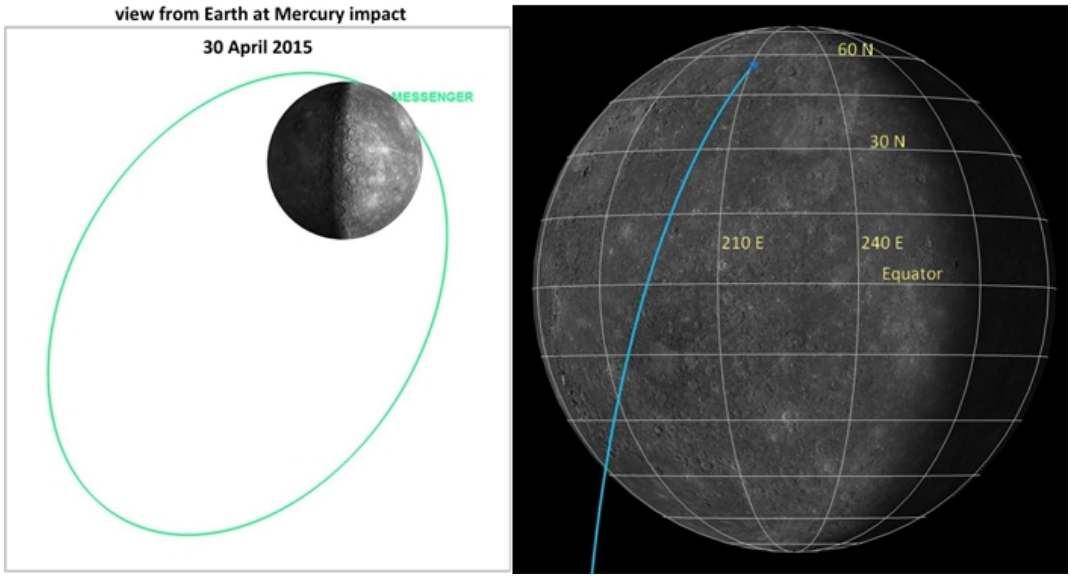

Figure 10. Views of MESSENGER’s Mercury Impact from Earth and above Mercury’s Equator

SUMMARY

After the successful completion of MESSENGER’s two-year second extended mission in mid-March of 2015 the project embarked on a six-week extension to XM2 that culminated in Mercury impact on 30 April 2015. With higher risk of early mission termination due to uncertainties in usable propellant and the effect of low-altitude Mercury gravity perturbations on the trajectory, the flight team completed five planned and two contingency OCMs in six weeks. During XM2′, the orbiter dropped four times to minimum altitudes of 5−9 km prior to the final descent to Mercury impact, for a total of five times closer to Mercury than the 11.7-km lowest XM2 phase altitude. The second half of XM2′ was enabled by the first-ever purposeful expulsion of helium pressurant to impart orbit-adjustment maneuvers. Successfully overcoming such challenges as rapid-cadence maneuver design-to-implementation (e.g., three OCMs in six days), substantial uncertainties in accessible propellant, and difficulty in meeting precise requirements for orbit determination at extremely low altitude led to novel scientific advances in understanding Mercury’s crustal magnetic field and water-ice deposits within permanently shadowed craters.

ACKNOWLEDGMENTS

The authors acknowledge support by the NASA Discovery Program Office throughout all phases of the MESSENGER mission. We thank Catherine Johnson for providing Figure 4. The authors are grateful for the key contributions of former Navigation Team Chief Tony Taylor of KinetX Aerospace for his ongoing Mercury gravity field updates and final reconstructed ephemeris solutions for MESSENGER.

REFERENCES

[1] J. V. McAdams, D. P. Moessner, K. E. Williams, A. H. Taylor, B. R. Page, and D. J. O’Shaughnessy, “MESSENGER – Six Primary Maneuvers, Six Planetary Flybys, and 6.6 Years to Mercury Orbit,” *Astrodynamics 2011: Part III, Advances in the Astronautical Sciences,* Vol. 142, pp. 2191–2210, 2012.

[2] D. P. Moessner and J. V. McAdams, "The MESSENGER Spacecraft's Orbit-Phase Trajectory," *Astrodynamics 2011: Part III, Advances in the Astronautical Sciences,* Vol. 142, pp. 2211–2230, 2012.

[3] J. V. McAdams, C. G. Bryan, D. P. Moessner, B. R. Page, D. R. Stanbridge, and K. E. Williams, "Orbit Design and Navigation through the End of MESSENGER's Extended Mission at Mercury," *Space Flight Mechanics 2014: Part III, Advances in the Astronautical Sciences,* Vol. 152, pp. 2299–2318, 2014.

[4] B. R. Page, C. G. Bryan, K. E. Williams, A. H. Taylor, and B. G. Williams, "Tuning the MESSENGER State Estimation Filter for Controlled Descent to Mercury Impact," *Astrodynamics Specialist Conference: American Institute of Aeronautics and Astronautics/American Astronautical Society,* paper AIAA-2014-4129, 16 pp., San Diego, CA, August 4-7, 2014.

[5] S. H. Flanigan, M. N. Kirk, D. J. O'Shaughnessy, S. S. Bushman, and P. E. Rosendall, "The First Three Maneuvers during MESSENGER's Low-Altitude Science Campaign." *38th Guidance and Control Conference, American Astronautical Society,* paper AAS 15-137, 12 pp., Breckenridge, CO, January 30 – February 4, 2015.

[6] D. P. Moessner and J. V. McAdams, "Design, Implementation, and Outcome of MESSENGER's Trajectory from Launch to Mercury Impact." *Astrodynamics Specialist Conference, American Astronautical Society/American Institute of Aeronautics and Astronautics,* paper AAS 15-634, 20 pp., Vail, CO, August 10 – 13, 2015.

[7] J. C. Leary, R. F. Conde, G. Dakermanji, C. S. Engelbrecht, C. J. Ercol, K. B. Fielhauer, D. G. Grant, T. J. Hartka, T. A. Hill, S. E. Jaskulek, M. A. Mirantes, L. E. Mosher, M. V. Paul, D. F. Persons, E. H. Rodberg, D. K. Srinivasan, R. M. Vaughan, and S. R. Wiley, "The MESSENGER Spacecraft," *Space Science Reviews,* Vol. 131*,* pp. 161–186, 2007.

[8] B. J. Anderson, C. L. Johnson, H. Korth, R. M. Winslow, J. E. Borovsky, M. E. Purucker, J. A. Slavin, S. C. Solomon, M. T. Zuber, and R. L. McNutt, Jr., "Low-Degree Structure in Mercury's Planetary Magnetic Field," *Journal of Geophysical Research*, Vol. 117, E00L12, 10.1029/2012JE004159, 2012.

[9] C. L. Johnson, M. E. Purucker, H. Korth, B. J. Anderson, R. M. Winslow, M. M. H. Al Asad, J. A. Slavin, I. I. Alexeev, R. J. Phillips, M. T. Zuber, and S. C. Solomon, "MESSENGER Observations of Mercury's Magnetic Field Structure," *Journal of Geophysical Research*, Vol. 117, E00L14, 10.1029/2012JE004217, 2012.

[10] H. Korth, N. A. Tsyganenko, C. L. Johnson, L. C. Philpott, B. J. Anderson, M. M. A. Asad, S. C. Solomon, and R. L. McNutt, Jr., "Modular Model for Mercury's Magnetospheric Magnetic Field Confined Within the Average Observed Magnetopause," *Journal of Geophysical Research Space Physics*, Vol. 120, in press, 10.1002/2015JA021022, 2015.

[11] C. L. Johnson, R. J. Phillips, M. E. Purucker, B. J. Anderson, P. K. Byrne, B. W. Denevi, J. M. Feinberg, S. A. Hauck, J. W. Head, H. Korth, P. B. James, E. Mazarico, G. A. Neumann, L. C. Philpott, M. A. Siegler, N. A. Tsyganenko, and S. C. Solomon, "Low-Altitude Magnetic Field Measurements by MESSENGER Reveal Mercury's Ancient Crustal Field," *Science*, Vol. 348, pp. 892–895, 10.1126/science.aaa8720, 2015.

[12] N. L. Chabot, C. M. Ernst, B. W. Denevi, H. Nair, A. N. Deutsch, D. T. Blewett, S. L. Murchie, G. A. Neumann, E. Mazarico, D. A. Paige, J. K. Harmon, J. W. Head, and S. C. Solomon, "Images of Surface Volatiles in Mercury's Polar Craters Acquired by the MESSENGER Spacecraft," *Geology*, Vol. 42, 1051−1054, 10.1130/G35916.1, 2014.

[13] D. J. Lawrence, W. C. Feldman, J. O. Goldsten, S. Maurice, P. N. Peplowski, B. J. Anderson, D. Bazell, R. L. McNutt, L. R. Nittler, T. H. Prettyman, D. J. Rodgers, S. C. Solomon, and S. Z. Weider, "Evidence for Water Ice Near Mercury's North Pole from MESSENGER Neutron Spectrometer Measurements," *Science*, Vol. 339, pp. 292−296, 10.1126/science.1229953, 2013.

[14] J. M. Raines, D. J. Gershman, J. A. Slavin, T. H. Zurbuchen, H. Korth, B. J. Anderson, and S. C. Solomon, "Structure and Dynamics of Mercury's Magnetospheric Cusp: MESSENGER Measurements of Protons and Planetary Ions," *Journal of Geophysical Research Space Physics*, Vol. 119, pp. 6587–6602, 10.1002/2014ja020120, 2014.

[15] G. P. Sutton, and O. Biblarz, "Rocket Propulsion Elements," 8th ed., Wiley, Hoboken, NJ, p. 267, 2010.

[16] S. R. Wiley, K. Dommer, C. S. Engelbrecht, and R. M. Vaughan, "MESSENGER Propulsion System Flight Performance," Paper AIAA-2006-4689, *42nd American Institute of Aeronatics and Astronautics/American Society of Mechanical Engineers/Society of Automotive Engineers/American Society of Electrical Engineers Joint Propulsion Conference and Exhibit*, Sacramento, CA, 9–12 July 2006.

[17] D. R. Stanbridge, K. E. Williams, A. H. Taylor, B. R. Page, C. G. Bryan, B. G. Williams, and D. W. Dunham, "Achievable Force Model Accuracies for MESSENGER in Mercury Orbit," *Astrodynamics 2011: Part III, Advances in the Astronautical Sciences,* Vol. 142, pp. 2231–2250, 2012.